Journal of Biological Physics (2022) 48:237–251
https://doi.org/10.1007/s10867-022-09608-w

ORIGINAL PAPER

Interaction among bovine serum albumin (BSA) molecules in the presence of anions: a small-angle neutron scattering study

Subhankar Pandit[1] · **Sarathi Kundu**[1] · **Vinod K. Aswal**[2]

Received: 7 December 2021 / Accepted: 30 March 2022 / Published online: 13 April 2022

Abstract
Protein–protein interaction in solution strongly depends on dissolved ions and solution pH. Interaction among globular protein (bovine serum albumin, BSA), above and below of its isoelectric point (pI ≈ 4.8), is studied in the presence of anions (Cl^-, Br^-, I^-, F^-, SO_4^{2-}) using small-angle neutron scattering (SANS) technique. The SANS study reveals that the short-range attraction among BSA molecules remains nearly unchanged in the presence of anions, whereas the intermediate-range repulsive interaction increases following the Hofmeister series of anions. Although the interaction strength modifies below and above the pI of BSA, it nearly follows the series.

Keywords Bovine serum albumin · Protein–protein interaction · Small-angle neutron scattering · Isoelectric point · Effect of anions

1 Introduction

Protein stability in solution and the related protein–protein interactions are the fundamental aspects of different biological applications [1, 2]. Globular proteins, e.g., bovine serum albumin (BSA), human serum albumin (HSA), lysozyme, etc. are charged colloidal particles [3, 4]. Depending upon the solution pH and isoelectric point (pI) of a particular protein, the net surface potential of protein changes, which influences the related interactions [5, 6]. The protein–protein interactions highly depend on protein concentration, pH, temperature, dissolved ions, and ionic strength [7–10]. Depending upon these parameters, various protein interactions such as protein crystallization, liquid–liquid phase separation, aggregation, and re-entrant condensation can be observed [11–14]. Among these different influencing factors, the nature of ions and their concentration highly influence the protein–protein interactions. A significant instability and stress can be observed in the living systems due to imbalance

✉ Sarathi Kundu
sarathi.kundu@gmail.com

[1] Soft Nano Laboratory, Physical Sciences Division, Institute of Advanced Study in Science and Technology, Vigyan Path, Paschim Boragaon, Assam 781035 Garchuk, Guwahati, India

[2] Solid State Physics Division, Bhabha Atomic Research Centre, Mumbai 400 085, India

of salts [15]. The effect of ions on protein–protein interactions can be predicted from the Hofmeister series, which are categorized as direct and reverse [16–19]. Depending on salt concentration as well as solution pH, proteins may follow different Hofmeister series [20]. It is evident that the Coulombic and van der Waals interactions between protein lead to the different phase behaviours of the protein in solution [21, 22]. Some non-specific interactions, namely hydrophobic interactions, entropic contribution, and hydration forces, may also play a significant role in the interactions [23, 24].

The interaction among proteins in solution and related equilibrium phase behaviour can be explained using the well-known Derjaguin-Landau-Verwey-Overbeek (DLVO) theory [25, 26]. Traditionally, the DLVO theory works well in low ionic concentrations; however, at higher salt concentration, the theory is validated by using effective interaction parameters [26, 27]. This theory cannot describe the rich and complex phase behaviour of proteins completely, due to its surface charge distribution as well as complex structure [3, 28]. Therefore, along with this theoretical model, few experimental methods, e.g. small-angle X-ray scattering (SAXS), small-angle neutron scattering (SANS), and dynamic light scattering (DLS), are also utilized to explain the interactions among proteins in solution [29, 30]. In the scattering study, the structure of protein can be predicted from the form factor, whereas interaction nature can be explained by studying the structure factor obtained from scattering intensity [29, 31]. In the SANS study, Yukawa potentials were also utilized in many cases to explain the interaction nature, which include the short-range attractive interactions, intermediate-range electrostatic repulsive interactions, and weak long-range attractive interactions [30, 32–34]. The protein–protein interactions can largely be affected by the charge of ions and can show phase separation behaviour in the presence of few ions [34, 35]. Effective interactions among BSA molecules enhance by replacing Cl^- ions with NO^{3-} ions [36]. The intermolecular interaction potential, specifically the attractive potential of lysozyme, shows pressure-dependent variation in the presence of anions [37]. Microstructural properties of protein gels also have an anion effect and follow the Hofmeister series partially [38]. Although a substantial study has been done using several experimental techniques and theoretical models to understand the protein–protein interactions in solution, further study is still essential for proper understanding of such complex systems.

Here, structure and interaction behaviour among BSA molecules are investigated in the presence of different anionic environment using SANS techniques. Interaction behaviours are studied in the presence of anions, namely, Cl^-, F^-, I^-, Br^-, and SO_4^{2-} ions, both above and below of the *p*I of BSA protein (*p*I ≈ 4.8). Using the two-Yukawa potential, the attractive and repulsive interactions among the BSA molecules were extracted. The relative strengths of the interactions with the concentration of salt are also explored. It is observed that, though the short-range attractive interactions remain nearly unchanged, the intermediate-range repulsive interactions vary in the presence of different anions. The variation of interactions is slightly modified depending on the solution pH above and below of the BSA *p*I but roughly follows the Hofmeister series of anions.

2 Materials and methods

BSA (catalogue No. 05480) was procured from Fluka and was used as received. For the SANS experiments, BSA samples were prepared using the buffer solution of D_2O. The final solution of BSA for all the measurements was fixed at 10 wt%. The *p*D of the sample was adjusted for two conditions at around 7.0 and 4.0, respectively, in 20 mM acetate

buffer in D_2O. The protein interactions in the presence of anions were studied by dissolving sodium chloride (NaCl), sodium fluoride (NaF), sodium bromide (NaBr), sodium iodide (NaI), and sodium sulphate (Na_2SO_4) salts in the protein solution. Two different salt concentrations were considered, i.e. 120 and 250 mM. SANS experiments were performed at Dhruva Reactor of Bhabha Atomic Research Centre (BARC), Mumbai [39]. The wavelength of the incident neutron beam (λ) was of 5.2 Å with a resolution ($\Delta\lambda/\lambda$) of ≈ 15%. All the data were collected in the scattering vector (Q) range of 0.017–0.35 $Å^{-1}$. The scattered neutrons were detected using a 100 cm long, 3.8 cm diameter position-sensitive gas detector. Standard procedures are used to correct and normalize the collected SANS data to a cross-sectional unit. Experimental temperature was 25 °C. At the end of final data fitting, the individual error for each parameter was evaluated.

3 SANS analysis

The SANS analysis was done using our earlier study [30, 33]. The intensity of the scattered neutron beam, $I(Q)$, is obtained from the SANS experiment. The scattering vector Q can be defined as $\frac{4\pi}{\lambda}\sin\theta$, where the scattering angle is 2 θ. The absolute scattering intensity for a system of monodisperse particles can be written as [40]:

$$I(Q) = n_p V_p^2 \left(\rho_p - \rho_s\right)^2 P(Q) S(Q) + B \tag{1}$$

where the protein molecule's number density in solution is denoted by n_p and V_p is the protein molecular volume. The scattering length density of the protein molecules is denoted by ρ_p and that of solvent is denoted by ρ_s. After orientation averaging, the scattering from a single protein molecule, i.e. the normalized form factor, is indicated by $P(Q)$. In our analysis, a form factor of oblate ellipsoid was considered to model the BSA molecule [9, 30]. The structure factor and the incoherent background, which is a constant, are represented by $S(Q)$ and B, respectively. The two-Yukawa potential (U_{TY}) with the mean spherical approximation (MSA) was used to calculate $S(Q)$. The ellipsoidal protein molecules are considered a rigid sphere of diameter, $\sigma = 2(ab^2)^{1/3}$ where the semi-major and semi-minor axes of the ellipsoidal protein molecules are respectively denoted by a and b. Furthermore, using the U_{TY} model [32, 41], the short-range attractive force and repulsive long-range force between the protein molecules are described. The potential model can be described as:

$$U_{TY}(r) = \begin{cases} \infty \; for \; r < 1 \\ -K_1 \frac{\exp\left[-Z_1(r-1)\right]}{r} - K_2 \frac{\exp\left[-Z_2(r-1)\right]}{r} for \; r \geq 1 \end{cases} \tag{2}$$

where r is the interparticle distance normalized by σ, the diameter of the particle. K_1 and K_2 are k_BT normalized interactions, where k_B and T are the Boltzmann constant, and absolute temperature, respectively. For attractive interactions, K_1, K_2 become positive, whereas for repulsive interactions, the values become negative. In our analysis, obtained K_1 and K_2 values are positive and negative, respectively. The specific interaction range is inversely proportional to Z. The short-range attractive interaction is basically a van der Waals interaction among two neighbouring molecules, which is effective in a very short distance (few Angstroms, typically 0–6 Å), and the energy varies as $1/r$ (where r is the inter molecular distance); however, the magnitude of interaction or Hamaker constant associated with it is

relatively small, and therefore at large distance, it has no effect. The long-range interaction between the same charged molecules is the electrostatic repulsion. The repulsive energy varies as $\frac{e^{-\kappa r}}{r}$ (where $1/\kappa$ is the Debye length) with an interaction constant. However, the magnitude of this interaction constant is relatively higher than the short-range attractive interaction. Typically, the effect of long-range repulsion can be observed from a few Å to up to some nanometre [4, 21, 42]. The charge of protein (z_p) and ionic strength (I) can be linked with the parameters K_2 and Z_2 using the DLVO theory [43]. The repulsive part of the Yukawa potential can be related with the screened Coulomb repulsion as

$$\frac{z_p^2 e^2}{4\pi\varepsilon\varepsilon_0\sigma(1+\frac{\kappa\sigma}{2})^2} = K_2 k_B T \tag{3}$$

where e is the charge of the electron, ε is the dielectric constant of water, and z_p is the effective charge of protein (in e units) due to electrostatic screening. K_2 is the repulsive strength in U_{TY}, and T is the absolute temperature. The ionic strength (I) is related to Z_2, the inverse of the repulsive range, by

$$\frac{3}{\sqrt{I}} = \kappa^{-1} = \frac{\sigma}{Z_2};\ i.e., I = \frac{9Z_2^2}{\sigma^2} \tag{4}$$

The experimental data was analysed using IGOR Pro software selecting the specific model of scattering, where the macros were developed by the NIST Center for Neutron Research [44]. The nonlinear least-squares method was used for the optimization of the parameters [45]. The volume fraction, form factor, short- and long-range attractive and repulsive potential ranges, and background for pure BSA were initially constant to obtain the physically reasonable values of other fitting parameters. After that, all parameters were free during fitting excluding the form factor, volume fraction, short-range potential, and the background. The same procedure was followed for the case of protein in the presence of the salts. The effective structure factor was calculated using the effective sphere diameter (σ). The parameters except for which error will be calculated were fixed after the final data fitting, during error calculation. The individual error is calculated from the standard deviation of the data fitting.

4 Results

SANS data (open circle) and the corresponding fitted curves (solid line) for BSA solution at pD ≈ 7.0 are shown in Fig. 1a. The structure factor $S(Q)$, as obtained from the fitting of all the samples, is shown in Fig. 1b. The inset of the figure shows the form factor, $P(Q)$ of pure BSA. An oblate form factor of dimensions ($a \times b \times b$) ≈ 10.2×40.0×40.0 Å is used for pure BSA during fitting. Moreover, U_{TY} model was also used during data fitting. The SANS data (open circles) of BSA at the same pD and in the presence of different salts (NaI, NaBr, NaCl, NaF, and Na_2SO_4) at 120 mM concentration are shown in Fig. 1a, whereas corresponding fitted curves (solid lines) are also shown in the same figure. Almost the same form factor (≈ 9.8×40.0×40.0 Å) and the two-Yukawa potentials were used to study the variation of attractive and repulsive strength in the presence of different salts. The corresponding structure factor, $S(Q)$, of the samples as obtained from the data fitting is shown in Fig. 1b. In Table 1, the parameters corresponding to the data fitting are tabulated.

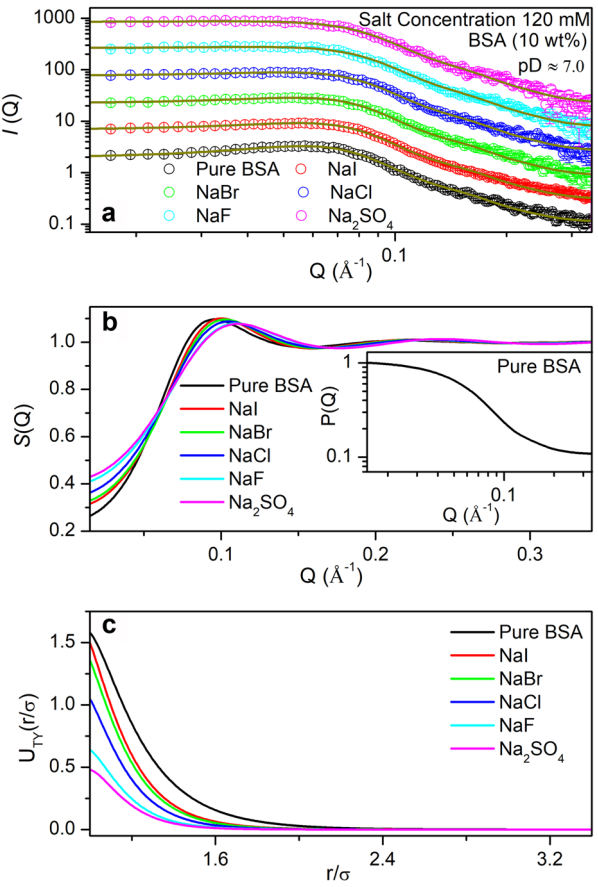

Fig. 1 **a** SANS data (open circle) for 10 wt% BSA and related fitted curves (solid line) in presence and absence of NaI, NaBr, NaCl, NaF, and Na_2SO_4, at 120 mM concentration in the aqueous solution at pD ≈ 7.0. Curves are shifted vertically for better visualization. **b** Structure factor, $S(Q)$, of the respective data, extracted from the data fitting using the U_{TY} model. Inset: Pure BSA form factor [$P(Q)$]. **c** Variation of U_{TY} as a function of the normalized intermolecular distance (r/σ)

Figure 1a shows that the scattering intensity varies in the low-Q region in the presence of different salts. The value of $I(Q)$ increases gradually, in the presence of NaI, NaBr, NaCl, NaF, and Na_2SO_4, respectively. It has a similarity with the Hofmeister series for anions [19]. The same nature is also reflected in the $S(Q)$ plots of Fig. 1b. From the $S(Q)$-Q plots as extracted from the data fitting, monomer–monomer correlation peak is observed. Figure 1c corresponds to the variation of U_{TY} as a function of r/σ (i.e. intermolecular distance normalized by the diameter σ of BSA) in the presence and absence of salt at 120 mM concentration. It is observed that in the presence of salts, the attractive interactions among protein remain almost the same, but the repulsive interaction strength increases. The order of strength enhancement depending upon the used anions is as follows: $I^- > Br^- > Cl^- > F^- > SO_4^{2-}$.

The SANS data of pure BSA and in the presence of above-mentioned salts at 250 mM salt concentration (open circles) are shown in Fig. 2a. The corresponding fitted curves are indicated in the same figure using solid lines. It is clear from the figure that, at low-Q region, the SANS intensity increases in the presence of salt as before. Nearly the same form factor for pure BSA (i.e. ≈ 9.8×40.0×40.0 Å) and same potential model, U_{TY}, was used during data fitting. The extracted values of repulsive and attractive strengths and the related parameters as obtained from the fitted data are showed in Table 2. The structure factor $S(Q)$

Table 1 Fitted parameters obtained from BSA solutions (10 wt%), in different solution *p*D, in the absence and presence of 120 mM salt concentrations, by using two-Yukawa potential model with a fixed volume fraction of 0.09. The charge is in electron (*e*) units, and diameter of BSA is in Å. The values shown inside the brackets indicate maximum errors of the fitted parameters

*p*D	Salt	K_1 (±0.06)	Z_1 (±0.1)	K_2 (±0.01)	Z_2 (±0.02)	*a* (in Å)	*b* (in Å)	2R (σ, in Å unit) (±0.2)	*I* (cal.)	*I* (expt.)	Charge (in e units) (±0.05)	*B*
7.0	No salt	0.7	11.5	−2.28	3.68	10.2	40	50.8	0.047	0.02	11.40	0.108
	NaI	0.7	11.5	−2.20	5.13	9.8	40	50.1	0.090	0.14	13.96	0.099
	NaBr	0.7	11.5	−2.06	5.31	9.8	40	50.1	0.101	0.14	13.85	0.095
	NaCl	0.7	11.5	−1.75	5.77	9.8	40	50.1	0.119	0.14	13.57	0.095
	NaF	0.7	11.8	−1.32	6.49	9.8	40	50.1	0.151	0.14	12.88	0.093
	Na_2SO_4	0.7	11.8	−1.16	6.82	9.8	40	50.1	0.168	0.38	12.54	0.090
4.0	No salt	0.7	11.5	−1.56	3.58	11.8	41.5	54.6	0.039	0.02	9.60	0.100
	NaI	0.7	11.5	−1.54	4.06	10	40	50.4	0.058	0.14	9.96	0.082
	NaBr	0.7	11.5	−1.30	4.47	10	40	50.4	0.071	0.14	9.77	0.078
	NaCl	0.7	11.5	−1.14	4.77	10	40	50.4	0.081	0.14	9.57	0.083
	NaF	0.7	11.8	−0.80	5.16	10	40	50.4	0.094	0.14	8.48	0.070
	Na_2SO_4	0.7	11.5	−0.75	5.64	10	40	50.4	0.113	0.38	8.76	0.095

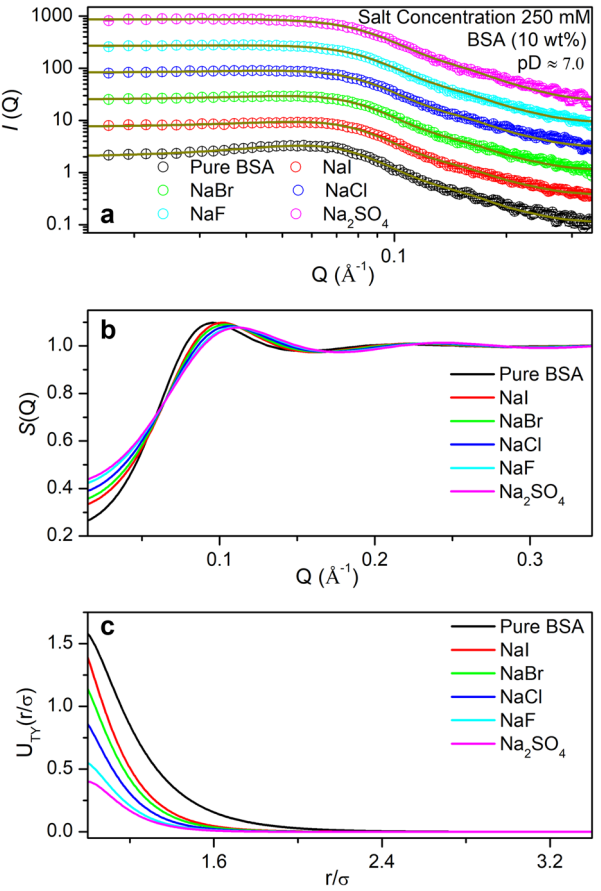

Fig. 2 **a** SANS data (open circle) for 10 wt% BSA and related fitted curves (solid line) in the presence of NaI, NaBr, NaCl, NaF, and Na_2SO_4, at 250-mM concentration in the aqueous solution at *p*D ≈ 7.0. Curves are shifted vertically for better visualization. **b** Structure factor, $S(Q)$, of the respective data as obtained from the data fitting using the U_{TY} model. **c** Variation of U_{TY} of every sample as a function of the normalized distance (r/σ)

and the variation of U_{TY} as a function of r/σ are plotted in Fig. 2b and c, respectively. In the presence of salt, the attractive interactions among protein molecules remain almost the same, whereas the repulsive interactions decrease gradually for I^-, Br^-, Cl^-, F^-, and SO_4^{2-}. From Table 2, it is also observed that the repulsive interaction strength decreases with the increment of salt concentration. This may be due to the electrostatic screening which leads to such enhancement of attractive interaction strength [34].

The *p*H effect on the interaction nature among proteins in the presence of anions is also investigated. Below the isoelectric point (*p*I ≈ 4.8), BSA possess net positive charge, and therefore, the interaction behaviour is studied at *p*D ≈ 4.0. The SANS profile of BSA (open circle) at *p*D ≈ 4.0 is shown in Fig. 3a, whereas the solid lines correspond to fitted curve. The $S(Q)$, obtained from the corresponding fitting, is shown in Fig. 3b. BSA form factor $P(Q)$ at that *pD* is shown in the inset of the figure. To fit the data, a form factor of oblate ellipsoid of dimensions ($a \times b \times b$) ≈ 11.8×41.5×41.5 Å and the same potential model (U_{TY}) was utilized. The SANS profiles (open circles) of BSA at the same *p*D in the presence of previously mentioned salts with 120 mM concentration are plotted in Fig. 3a. Solid lines of the figure correspond to the fitted curves for the respective samples. To study the variation of attractive and repulsive strength in the presence of different salts, form factor of dimension ≈ 10×40.0×40.0 Å and U_{TY} potential model were used. The obtained

Table 2 Fitted parameters obtained from BSA solutions (10 wt%), in different solution *p*D, in the absence and presence of 250 mM salt concentrations, by using two-Yukawa potential model with fixed volume fraction of 0.09. The charge is in electron (*e*) units, and diameter of BSA is in Å. The values shown inside the brackets indicate maximum errors of the fitted parameters

*p*D	Salt	K_1 (±0.06)	Z_1 (±0.1)	K_2 (±0.01)	Z_2 (±0.02)	*a* (in Å)	*b* (in Å)	2R (σ, in Å unit) (±0.2)	*I* (cal.)	*I* (expt.)	Charge (in e unit) (±0.05)	*B*
7.0	No salt	0.7	11.5	−2.28	3.68	10.2	40	50.8	0.047	0.02	11.40	0.108
	NaI	0.7	11.5	−2.07	5.56	9.8	40	50.1	0.111	0.27	14.36	0.120
	NaBr	0.7	11.5	−1.84	5.80	9.8	40	50.1	0.121	0.27	13.97	0.120
	NaCl	0.7	11.5	−1.56	6.32	9.8	40	50.1	0.143	0.27	13.72	0.110
	NaF	0.7	11.5	−1.25	6.78	9.8	40	50.1	0.165	0.27	12.96	0.110
	Na_2SO_4	0.7	11.5	−1.10	6.96	9.8	40	50.1	0.174	0.77	12.41	0.095
4.0	No salt	0.7	11.5	−1.56	3.58	11.8	41.5	54.6	0.039	0.02	9.60	0.100
	NaI	0.7	11.5	−1.48	4.53	10	40	50.4	0.073	0.27	10.52	0.095
	NaBr	0.7	11.5	−1.29	4.73	10	40	50.4	0.079	0.27	10.12	0.090
	NaCl	0.7	11.5	−1.01	5.45	10	40	50.4	0.105	0.27	9.91	0.085
	NaF	0.7	11.5	−0.78	5.79	10	40	50.4	0.119	0.27	9.11	0.093
	Na_2SO_4	0.7	11.5	−0.68	5.83	10	40	50.4	0.120	0.77	8.55	0.090

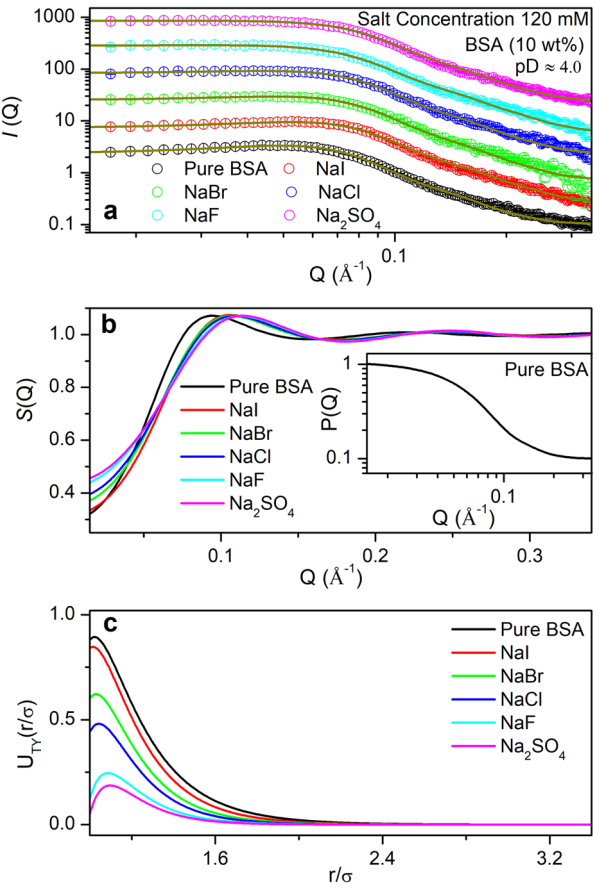

Fig. 3 **a** SANS data (open circle) for 10 wt% BSA in absence and presence of NaI, NaBr, NaCl, NaF, and Na_2SO_4, at 120 mM concentration in the aqueous solution at pD ≈ 4.0 and related fitted curves (solid line). Curves are shifted vertically for better visualization. **b** Structure factor, $S(Q)$, of the respective data, obtained from the fitting using the U_{TY} model. Form factor $P(Q)$ for pure BSA at pD ≈ 4.0 is at inset. **c** Variation of U_{TY} of every sample as a function of the normalized distance (r/σ)

parameters after fitting are tabulated in Table 1. The structure factor, $S(Q)$, corresponding to the samples is also shown in Fig. 3b, whereas Fig. 3c corresponds to the variation of U_{TY} as a function of r/σ. From the figure, it is cleared that, at low-Q value, the SANS profile increases gradually, almost the similar tend as followed at pD ≈ 7.0. Though, the profile for BSA in the presence of NaI salt is almost similar with pure BSA. Moreover, in the presence of NaF and Na_2SO_4, the SANS profiles of BSA are almost similar. The order intensity profiles of BSA in the presence of salts are as follows: No salt ≈ $I^- < Br^- < Cl^- < F^-$ ≈ $SO4^{2-}$. In this experimental condition also, the relative strength of attraction almost remains constant, but the strength of repulsion decreases gradually as follows: I^-, Br^-, Cl^-, F^-, and SO_4^{2-}.

The SANS data of BSA in the absence and presence of the above-mentioned salts at pD ≈ 4.0, for 250 mM concentrations (open circles), are shown in Fig. 4a, whereas the solid lines of the same figure correspond to the fitted curves. A similar form factor of ≈ 10×40.0×40.0 Å is used for pure BSA during fitting, whereas the U_{TY} model is utilized to fit the scattering data. It is observed that, at low-Q region, the SANS intensity increases depending up on the salts as found in the presence of 120 mM salt at pD ≈ 4.0. The extracted values of attractive and repulsive strengths and related parameters from the fitting are shown in Table 2. The structure factor $S(Q)$ and the variation of U_{TY} with respect to r/σ are shown in Fig. 4b and c, respectively. In this condition also, the strength of short-range

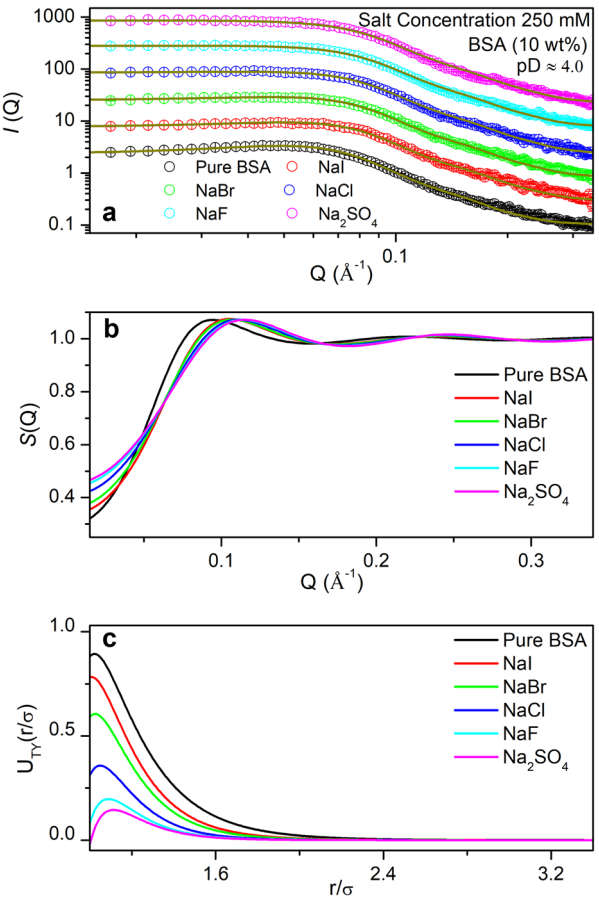

Fig. 4 **a** SANS data (open circle) for 10 wt% BSA at pD ≈ 7.0 in the absence and presence of NaI, NaBr, NaCl, NaF, and Na_2SO_4, at 250 mM concentration in the aqueous solution and related fitted curves (solid line). Curves are shifted vertically for better visualization. **b** Structure factor, $S(Q)$, extracted from the data fitting using the (U_{TY}) model. **c** Variation of the U_{TY} of the samples as a function of the normalized distance (r/σ)

attraction remains nearly constant, whereas the strength of long-range repulsion decreases following the order as mentioned previously, i.e. strength is maximum and minimum for NaI and Na_2SO_4, respectively. It is also found that the strength of the repulsive interactions is lowered at higher salt concentration for a particular solution pD. The repulsive strength of BSA for a particular salt is also decreased at pD ≈ 4.0 than pD ≈ 7.0.

5 Discussion

Proteins typically have a net surface charge. However, the interactions of proteins with specific ions and the ion cloud distribution over the protein are not easy to predict. In the presence of ions, a charge screening is observed among the charged protein molecules. The net effects of short-range and long-range interactions determine different phase behaviours of protein solutions. The dominating behaviour of short-range attraction is responsible for different phase separation behaviours such as liquid–liquid phase separation (LLPS), re-entrant condensation (RC), and protein crystallization. An effective short-range attraction over long or intermediate range repulsions is observed in the RC behaviour of globular proteins in

the presence of tri- and tetra-valent ions [35, 46]. In case of metastable LLPS, the effective attraction among proteins is shorter than the size of the particles [47]. From the results as obtained from the SANS analysis, it is clear that the interactions among BSA molecules modifies in the presence of anions and also with ion concentrations. In addition to this, the effective interaction changes with the solution *p*D. As discussed before, it is observed that the strength of short-range attraction (K_1) remains almost constant, but the intermediate range repulsive strength (K_2) varies with the presence of different anions. The variations of K_2 in the presence of anions for both the salt concentrations and at two solution *p*D conditions, i.e. above (*p*D ≈ 7.0) and below (*p*D ≈ 4.0), the isoelectric point of BSA are shown in Fig. 5a and c, respectively. Depending on the isoelectric point, BSA possesses net negative surface potential at *p*D ≈ 7.0. Though the Na^+ ions are present in the solution and are responsible for charge screening, the anions present in the solution interact with the positively charged side chains of BSA molecules. It is observed that the attractive short-range potential remains nearly unchanged, but the long-range repulsion potential decreases from I^- to SO_4^{2-}. Therefore, the effective strength of attraction becomes larger in the presence of SO_4^{2-}, and these ions interact more with the BSA molecules. Probably, due to the higher valency, the SO_4^{2-} ions show strong electrostatic interactions than the monovalent anions. For the monovalent anions, charge density follows as $I^- < Br^- < Cl^- < F^-$, and the effective strength of interactions among proteins also follows the same trend. Due to more interaction in the presence of F^- among all the monovalent anions, the effective charge of protein (z_p) is also reduced. The variations of z_p in the presences of the salts are shown in Fig. 5b and d, respectively, for *p*D ≈ 7.0 and 4.0. Therefore, the interactions among protein molecules in the presence of anions effectively follows a series such as $I^- < Br^- < Cl^- < F^- < SO_4^{2-}$, which is nothing but the Hofmeister series of anions. Similarly, at *p*D ≈ 4.0, also the same series is followed. At this *p*D, i.e. below the isoelectric point, protein shows net positive surface potential. Therefore, the effective strength of attraction becomes larger than in the case of *p*D ≈ 7. Thus, the surface charge density, relative binding strength, and the valency of ions

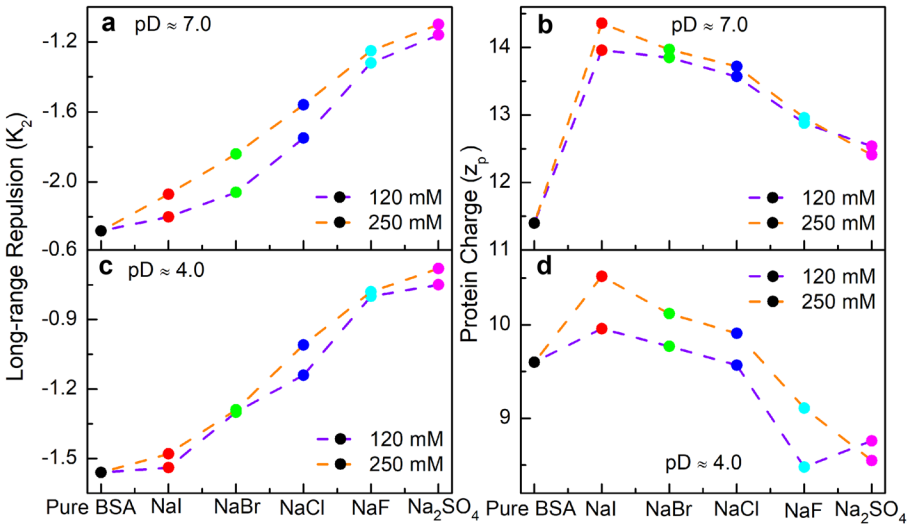

Fig. 5 Variation of K_2 (**a** and **c**) as extracted from the data fitting using the U_{TY} model and effective charge (z_p) (**c** and **d**) of BSA in the presence for different salts at around (**a** and **b**) *p*D 7.0 and (**c** and **d**) *p*D 4.0

play an important role in modifying the protein–protein interactions. The kosmotropic and chaotropic effects of salts can also be related with these interactions. Kosmotropic ions stabilize the protein structure by promoting the degree of hydrogen bonding in solution, whereas chaotropic ions disrupt the hydrogen bonding network and destabilize the protein structure [48, 49]. Therefore, in the presence of kosmotropes, the interactions among proteins in solution will be stronger. SO_4^{2-} is a well-known kosmotropes from Hofmeister series and shows more effective attraction. In case of chaotropic anions such as I^- and Br^-, the interactions are relatively weaker. Therefore, the protein–protein interactions may follow a more general series such as (chaotropic) $I^- < Br^- < Cl^- < F^- < SO_4^{2-}$ (kosmotropic).

In conclusion, BSA is a well-known and widely used model protein to study both protein–protein interactions and protein-salt interactions due to its abundance and similarity with human serum albumin. We have used five different anions, I^-, Br^-, Cl^-, F^-, and SO_4^{2-}, to study the interactions among BSA molecules both above and below the *p*I value of BSA. The short-range attraction among protein molecules remains nearly unchanged, whereas the intermediate range repulsive interactions decrease as $I^- > Br^- > Cl^- > F^- > SO_4^{2-}$. With the variation of solution *p*D, the interactions follow the same trend, but the decrement of repulsive strength is larger for BSA below the *p*I value of BSA, i.e., at *p*D $\approx$ 4.0. The interactions among the protein molecules, in the presence of anions, follow the Hofmeister series of anions, and the surface charge density and valency of anions play a crucial role in such interaction behaviour. This interaction study may be helpful to have a quantitative description and to understand the effect of anions on protein–protein interaction. However, actually it is a simplified model to explain such complex system only with the short-range or long-range interactions. There are some other factors, e.g., ion adoption, chaotropic effect, hydrophobic effect, hydration effect, and hydrogen bonding, which may also play some important roles in such protein-ion system and therefore need further investigation.

Acknowledgements SP acknowledges the Department of Science and Technology, Govt. of India, for the financial support through INSPIRE Fellowship (IF 160402). SK acknowledges financial support from the Department of Science and Technology, Govt. of India. Both the authors acknowledge IASST, Guwahati, for the financial and other experimental facilities.

Author contribution SP, SK, and VKA performed all the experiments, analysed the data, and wrote the manuscript. SK and VKA validated and supervised the work. All approved the manuscript.

Funding SP obtained the financial support through INSPIRE Fellowship (Grant no. IF 160402) supported by the Department of Science and Technology, Govt. of India.

Data availability Not applicable.

Code availability Not applicable.

Declarations

Conflict of interest The authors declare no competing interests.

References

1. Pasquier, C., Vazdar, M., Forsman, J., Jungwirth, P., Lund, M.: Anomalous protein−protein interactions in multivalent salt solution. J. Phys. Chem. B **121**, 3000–3006 (2017). https://doi.org/10.1021/acs.jpcb.7b01051

2. Keskin, O., Gursoy, A., Ma, B., Nussinov, R.: Principles of protein−protein interactions: what are the preferred ways for proteins to interact? Chem. Rev. **108**, 1225–1244 (2008). https://doi.org/10.1021/cr040409x
3. Piazza, R.: Protein interactions and association: an open challenge for colloid science. Curr. Opin. Colloid Interface Sci. **8**, 515–522 (2004). https://doi.org/10.1016/j.cocis.2004.01.008
4. Israelachvili, J.N.: Intermolecular and Surface Forces. Academic Press, USA (2011)
5. Barbosa, L.R.S., Ortore, M.G., Spinozzi, F., Mariani, P., Bernstorff, S., Itri, R.: The Importance of protein-protein interactions on the ph-induced conformational changes of bovine serum albumin: a small-angle X-ray scattering study. Biophys. J . **98**, 147–157 (2010). https://doi.org/10.1016/j.bpj.2009.09.056
6. Bostrom, M., Tavares, F.W., Finet, S., Skouri-panet, F., Tardieu, A., Ninham, B.W.: Why forces between proteins follow different Hofmeister series for pH above and below pI. Biophys. Chem. **117**, 217–224 (2005). https://doi.org/10.1016/j.bpc.2005.05.010
7. Matsarskaia, O., Braun, M.K., Roosen-runge, F., Wolf, M., Zhang, F., Roth, R., Schreiber, F.: Cation-induced hydration effects cause lower critical solution temperature behavior in protein solutions. J. Phys. Chem. B **120**, 7731–7736 (2016). https://doi.org/10.1021/acs.jpcb.6b04506
8. Lonetti, B., Fratini, E., Chen, S.H., Baglioni, P.: Viscoelastic and small angle neutron scattering studies of concentrated protein solutions. Phys. Chem. Chem. Phys. **6**, 1388–1395 (2004). https://doi.org/10.1039/b316144g
9. Zhang, F., Skoda, M.W.A., Jacobs, R.M.J., Martin, R.A., Martin, C.M., Schreiber, F.: Protein interactions studied by SAXS: effect of ionic strength and protein concentration for BSA in aqueous solutions. J. Phys. Chem. B **111**, 251–259 (2007). https://doi.org/10.1021/jp0649955
10. Matsarskaia, O., Roosen-runge, F., Schreiber, F.: Multivalent ions and biomolecules: attempting a comprehensive perspective. Chem. Phys. Chem. **21**, 1742–1767 (2020). https://doi.org/10.1002/cphc.202000162
11. Schubert, R., Meyer, A., Baitan, D., Dierks, K., Perbandt, M., Betzel, C.: Real-time observation of protein dense liquid cluster evolution during nucleation in protein crystallization Cryst. Growth Des. **17**, 954–958 (2017). https://doi.org/10.1021/acs.cgd.6b01826
12. Sauter, A., Zhang, F., Szekely, N.K., Pipich, V., Sztucki, M., Schreiber, F.: Structural evolution of metastable protein aggregates in the presence of trivalent salt studied by (V)SANS and SAXS. J. Phys. Chem. B **120**, 5564–5571 (2016). https://doi.org/10.1021/acs.jpcb.6b03559
13. Zhang, F., Weggler, S., Ziller, M.J., Ianeselli, L., Heck, B.S., Hildebrandt, A., Kohlbacher, O., Skoda, M.W.A., Jacobs, R.M.J., Schreiber, F.: Universality of protein reentrant condensation in solution induced by multivalent metal ions. Proteins **78**, 3450–3457 (2010). https://doi.org/10.1002/prot.22852
14. Matsarskaia, O., Vela, S.D., Mariani, A., Fu, Z., Zhang, F., Schreiber, F.: Phase-separation kinetics in protein−salt mixtures with compositionally tuned interactions. J. Phys. Chem. B **123**, 1913–1919 (2019). https://doi.org/10.1021/acs.jpcb.8b10725
15. Nostro, P.L., Ninham, B.W.: Hofmeister phenomena: an update on ion specificity in biology. Chem. Rev. **112**, 2286–2322 (2012). https://doi.org/10.1021/cr200271j
16. Okur, H.I., Hladílkova, J., Rembert, K.B., Cho, Y., Heyda, J., Dzubiella, J., Cremer, P.S., Jungwirth, P.: Beyond the Hofmeister series: ion-specific effects on proteins and their biological functions. J. Phys. Chem. B **121**, 1997–2014 (2017). https://doi.org/10.1021/acs.jpcb.6b10797
17. Kunz, W., Henle, J., Ninham, B.W.: 'Zur Lehre von der Wirkung der Salze' (about the science of the effect of salts): Franz Hofmeister's historical papers. Curr. Opin. Colloid Interface Sci. **9**, 19–37 (2004). https://doi.org/10.1016/j.cocis.2004.05.005
18. Kunz, W., Nostro, P.L., Ninham, B.W.: The present state of affairs with Hofmeister effects. Curr. Opin. Colloid Interface Sci. **9**, 1–18 (2004). https://doi.org/10.1016/j.cocis.2004.05.004
19. Jordan, J.H., Gibb, C.L.D., Wishard, A., Pham, T., Gibb, B.C.: Ion−hydrocarbon and/or ion−ion interactions: direct and reverse Hofmeister effects in a synthetic host. J. Am. Chem. Soc. **140**, 4092–4099 (2018). https://doi.org/10.1021/jacs.8b00196
20. Zhang, Y., Cremer, P.S.: The inverse and direct Hofmeister series for lysozyme. Proc. Natl. Acad. Sci. USA **106**, 15249–15253 (2009). https://doi.org/10.1073/pnas.0907616106
21. Tardieu, A., Verge, A.L., Malfois, M., Bonneté, F., Finet, S., Riès-Kautt, M., Belloni, L.: Proteins in solution: from X-ray scattering intensities to interaction potentials. J. Cryst. Growth **196**, 193–203 (1999). https://doi.org/10.1016/S0022-0248(98)00828-8
22. Lund, M., Jungwirth, P.: Patchy proteins, anions and the Hofmeister series. J. Phys.: Condens. Matter **20**, 494218 (2008). https://doi.org/10.1088/0953-8984/20/49/494218
23. Bostrom, M., Parsons, D.F., Salis, A., Ninham, B.W., Monduzzi, M.: Possible origin of the inverse and direct Hofmeister series for lysozyme at low and high salt concentrations. Langmuir **27**, 9504–9511 (2011). https://doi.org/10.1021/la202023r

24. Newberry, R.W., Raines, R.T.: Secondary forces in protein folding. ACS Chem. Biol. **14**, 1677–1686 (2019). https://doi.org/10.1021/acschembio.9b00339
25. Crocker, J.C., Grier, D.G.: When like charges attract: the effects of geometrical confinement on long-range colloidal interactions. Phys. Rev. Lett. **77**, 1897–1900 (1996). https://doi.org/10.1103/PhysRevLett.77.1897
26. Bostrom, M., Williams, D.R.M., Ninham, B.W.: Specific ion effects: why DLVO theory fails for biology and colloid systems. Phys. Rev. Lett. **87**, 168103 (2001). https://doi.org/10.1103/PhysRevLett.87.168103
27. Platten, F., Valadez-Pérez, N.E., Castañeda-Priego, R., Egelhaaf, S.U.: Extended law of corresponding states for protein solutions. J. Chem. Phys. **142**, 174905 (2015). https://doi.org/10.1063/1.4919127
28. Pellicane, G., Costa, D., Caccamo, C.: Theory and simulation of short-range models of globular protein solutions. J. Phys.: Condens. Matter **16**, S4923–S4936 (2004). https://doi.org/10.1088/0953-8984/16/42/010
29. Chaudhuri, B.N.: Emerging applications of small angle solution scattering in structural biology. Protein Sci. **24**, 267–276 (2015). https://doi.org/10.1002/pro.2624
30. Kundu, S., Pandit, S., Abbas, S., Aswal, V.K., Kohlbrecher, J.: Structures and interactions among globular proteins above the isoelectric point in the presence of divalent ions: a small angle neutron scattering and dynamic light scattering study. Chem. Phys. Lett. **693**, 176–182 (2018). https://doi.org/10.1016/j.cplett.2018.01.022
31. Svergun, D.I., Koch, M.H.J.: Small-angle scattering studies of biological macromolecules in solution. Rep. Prog. Phys. **66**, 1735–1782 (2003). https://doi.org/10.1088/0034-4885/66/10/R05
32. Liu, Y., Fratini, E., Baglioni, P., Chen, W., Chen, S.: Effective long-range attraction between protein molecules in solutions studied by small angle neutron scattering. Phys. Rev. Lett. **95**, 118102 (2005). https://doi.org/10.1103/PhysRevLett.95.118102
33. Pandit, S., Kundu, S., Abbas, S., Aswal, V.K., Kohlbrecher, J.: Structures and interactions among lysozyme proteins below the isoelectric point in presence of divalent ions. Chem. Phys. Lett. **711**, 8–14 (2018). https://doi.org/10.1016/j.cplett.2018.09.021
34. Kundu, S., Das, K., Aswal, V.K.: Modification of attractive and repulsive interactions among proteins in solution due to the presence of mono-, di- and tri-valent ions. Chem. Phys. Lett. **578**, 115–119 (2013). https://doi.org/10.1016/j.cplett.2013.05.062
35. Kumar, S., Yadav, I., Ray, D., Abbas, S., Saha, D., Aswal, V.K., Kohlbrecher, J.: Evolution of interactions in the protein solution as induced by mono and multivalent ions. Biomacromol. **20**, 2123–2134 (2019). https://doi.org/10.1021/acs.biomac.9b00374
36. Braun, M.K., Sauter, A., Matsarskaia, O., Wolf, M., Roosen-Runge, F., Sztucki, M., Roth, R., Zhang, F., Schreiber, F.: Reentrant phase behavior in protein solutions induced by multivalent salts: strong effect of anions Cl^- versus NO^{3-}. J. Phys. Chem. B **122**, 11978–11985 (2018). https://doi.org/10.1021/acs.jpcb.8b10268
37. Moller, J., Grobelny, S., Schulze, J., Steffen, A., Bieder, S., Paulus, M., Tolan, M., Winter. R.: Specific anion effects on the pressure dependence of the protein–protein interaction potential. Phys. Chem. Chem. Phys. **16**, 7423–7429 (2014). https://doi.org/10.1039/c3cp55278k
38. Bowland, E.L., Foegedlng, E.A.: Effects of anions on thermally induced whey protein isolate gels. Food Hydrocolloids **9**, 47–56 (1995). https://doi.org/10.1016/S0268-005X(09)80193-8
39. Aswal, V.K., Goyal, P.S.: Small-angle neutron scattering diffractometer at Dhruva reactor. Curr. Sci. **79**, 947–953 (2000)
40. Hayter, J.B., Penfold, J.: Determination of micelle structure and charge by neutron small-angle scattering. Colloid & Polym. Sci. **261**, 1022–1030 (1983). https://doi.org/10.1007/BF01421709
41. Wu, J., Liu, Y., Chen, W., Cao, J., Chen, S.: Structural arrest transitions in fluids described by two Yukawa potentials. Phys. Rev. E **70**, 050401(R) (2004). https://doi.org/10.1103/PhysRevE.70.050401
42. Tardieu, A., Finet, S., Bonnete, F.: Structure of the macromolecular solutions that generate crystals. J. Cryst. Growth **232**, 1–9 (2001). https://doi.org/10.1016/S0022-0248(01)01053-3
43. Verwey, E.J.W., Overbeek, J.T.G.: Theory of the Stability of Lyophobic Colloids. Elsevier, Amsterdam (1948)
44. Kline, S.R.: Reduction and analysis of SANS and USANS data using IGOR Pro. J. Appl. Cryst. **39**, 895–900 (2006). https://doi.org/10.1107/S0021889806035059
45. Pedersen, J.S.: Analysis of small-angle scattering data from colloids and polymer solutions: modeling and least-squares fitting. Adv. Coll. Interface. Sci. **70**, 171–210 (1997). https://doi.org/10.1016/S0001-8686(97)00312-6

46. Zhang, F., Skoda, M.W.A., Jacobs, R.M.J., Zorn, S., Martin, R.A., Martin, C.M., Clark, G.F., Weggler, S., Hildebrandt, A., Kohlbacher, O., Schreiber, F.: Reentrant condensation of proteins in solution induced by multivalent counterions. Phys. Rev. Lett. **101**, 148101 (2008). https://doi.org/10.1103/PhysRevLett.101.148101
47. Zhang, F., Roth, R., Wolf, M., Roosen-Runge, F., Skoda, M.W.A., Jacobs, R.M.J., Sztucki, M., Schreiber, F.: Charge-controlled metastable liquid–liquid phase separation in protein solutions as a universal pathway towards crystallization. Soft Matter **8**, 1313–1316 (2012). https://doi.org/10.1039/c2sm07008a
48. Naseem, B., Arif, I., Jamal, M.A.: Kosmotropic and chaotropic behavior of hydrated ions in aqueous solutions in terms of expansibility and compressibility parameters. Arab. J. Chem. **14**, 103405 (2021). https://doi.org/10.1016/j.arabjc.2021.103405
49. Adebowale, Y.A., Adebowale, K.O.: The influence of kosmotropic and chaotropic salts on the functional properties of Mucuna pruriens protein isolate. Int. J. Biol. Macromol. **40**, 119–125 (2007). https://doi.org/10.1016/j.ijbiomac.2006.06.016